Field-Dependent Energy Barriers of Magnetic Néel Skyrmions in Ultrathin Circular Nanodots

A. Riveros,[1,*] F. Tejo,[2] J. Escrig,[3,4] K.Y. Guslienko,[5,6] and O. Chubykalo-Fesenko[2]

[1] *Escuela de Ingeniería, Universidad Central de Chile, 8330601 Santiago, Chile*
[2] *Instituto de Ciencias de Materiales de Madrid, 28049 Madrid, España*
[3] *Departamento de Física, Universidad de Santiago de Chile, 9170124 Santiago, Chile*
[4] *Center for the Development of Nanoscience and Nanotechnology, 9170124 Santiago, Chile*
[5] *División de Física de Materiales, Departamento Polímeros y Materiales Avanzados: Física, Química y Tecnología, Universidad del País Vasco, UPV/EHU, 20018 San Sebastián, España*
[6] *Ikerbasque, the Basque Foundation for Science, 48009 Bilbao, España*

(Received 15 March 2021; revised 18 June 2021; accepted 2 July 2021; published 29 July 2021)

We evaluate the field-dependent energy barriers associated with annihilation of a Néel skyrmion in ultrathin magnetic nanodots with interfacial Dzyaloshinskii-Moriya interaction. Three scenarios of the skyrmion annihilation are considered: expansion or contraction of the radius of the skyrmion and skyrmion escape through the dot boundary. For typical parameters of Co/Pt circular nanodots, we find that at zero magnetic field, the energy barrier associated with a displacement of the skyrmion core is always lower than that corresponding to its expansion or contraction. Importantly, the energy barrier value is small, so that the skyrmion in ultrathin dots is unstable versus thermal fluctuations at room temperature for a long time scale. However, we find that the skyrmion can be stabilized by an out-of-plane magnetic field applied parallel to its core. The increase of the energy barriers corresponds to a magnetic field interval, where skyrmions of small and large radius coexist and the large-core-radius skyrmion is more stable than the small one. In this field region, the skyrmion can be stable for hours before it is annihilated by thermal fluctuations escaping through the dot edge.

DOI: 10.1103/PhysRevApplied.16.014068

I. INTRODUCTION

Magnetic skyrmions have been proposed as building blocks for ultralow power-consumption devices and memories in information technology [1–5]. This idea comes from the topological protection of the skyrmion state, which promises a long-time stability of information bits. Indeed, in infinite thin magnetic films, the two-dimensional (2D) topological charge (skyrmion number) is a conserved quantity [6]. Therefore, a magnetization configuration with a nonzero 2D topological charge cannot be brought about by a continuous transformation to a uniform ground state with zero topological charge. However, this statement is only valid for infinite films. Moreover, the topological protection does not mean that a skyrmion configuration is the film ground state. It has been demonstrated that the Bloch and Néel skyrmions in infinite films can only be metastable [7] and thus they decay on a long time scale to the stable state by thermal activation over the energy barrier. This fact would not be important if the energy barriers separating the metastable and the stable states were high. Thus, for any skyrmion applications, it is important to ensure high energy barriers of the skyrmionic states. Experiments conducted on skyrmions in bulk samples demonstrate that the skyrmion state may decay over time [8].

For real device applications, skyrmions are most probably confined in magnetic stripes or dots. Recent calculations have shown that the confinement of magnetic skyrmions in circular dots favors their stabilization [9–14]. However, even in dots, most of the small-size skyrmions, such as those in Co/Pt multilayers, are actually metastable states [9,10]. It has been shown that thermal fluctuations deform a skyrmion [15] and that these perturbations may destroy it. Thus, the problem of long-time skyrmion thermal stability is also important for magnetic dots and stripes.

Long-term stability for any magnetization state (if two or more equilibrium configurations exist) is defined via the energy barrier (ΔE) that separates these states, using the Arrhenius-Néel law $f = f_0 \exp(-\Delta E/k_B T)$, where f is the switching frequency, f_0 is the so-called Arrhenius-Néel prefactor, k_B is the Boltzmann constant, and T is

*alejandro.riveros@ucentral.cl

the temperature. At room temperature $T_0 = 300$ K, for $\Delta E/k_B T_0 \simeq 25$, the configuration is considered stable for several hours, while if $\Delta E/k_B T_0 \simeq 50$, stability over a period of 20 years is expected. Thus, to know the thermal stability of the skyrmions, knowledge of the energy barriers that separate the skyrmion and the quasiuniform (or other) states is essential.

No systematic study of skyrmion thermal stability, i.e., of the energy barriers in magnetic dots, with the aim of searching for additional skyrmion stabilization versus thermal fluctuations, exists so far. This is mainly due to the fact that numerical calculation of energy barriers of strongly inhomogeneous magnetization configurations is a nontrivial problem because one should look for the saddle point in a multidimensional space with rotational degeneracy (i.e., two points can be joined in this multidimensional space in many ways—for example, by rotating a selected part of the spins in the clockwise direction and the remaining part in the anticlockwise one). One of the known methods is based on the nudged elastic band [16–21]. Here, typically two magnetization configurations are joined by a virtual spring and the maximum along the path should be found. The problem here is that several energy barriers separating the two configurations may exist in the multidimensional case, especially because the magnetization dynamics occurs on a sphere with degenerate directions of rotation. Thus, the initial path of the elastic band frequently defines the reversal barrier, which may be not the lowest one. Moreover, the maximum at the elastic band path may correspond to a higher-order extremum with more than one negative eigenvalue of the energy functional.

Nevertheless, in the case of skyrmions, at least three types of energy barriers have been found using this method [19,20]. One corresponds to the symmetric skyrmion collapse, the second is mediated by topological reorganization, and the third (frequently reported as the lowest one), corresponds to the skyrmion escape through the track or dot edge. A detailed analysis of the energy barriers, transition states, and configurational entropy has been evaluated for skyrmion collapse, escape, and annihilation at defects in Ref. [20], for a simple Heisenberg model with no magnetostatic interactions. It has been shown that the problem is even more complicated, since a higher energy barrier may be compensated by a high transition rate, leading to the lowest energy path [20]. A simpler constriction method has been used in Ref. [22] for skyrmions showing a very low energy barrier in a monoatomic Co/Pt layer. The problem with this method is that it projects the multidimensional space to a one-dimensional space, which can hide the lowest energy barrier [23]. Finally, the magnetic stability of skyrmion bits in atomic layers has been evaluated by Monte Carlo simulations [24]. In any case, it seems to be established that skyrmions in ultrathin films such as bilayers are unstable versus thermal fluctuations and, in order to stabilize them, the multilayers strategy (i.e., additional magnetic material volume in the out-of-plane direction) is used [25,26].

The above discussion indicates that the problem of determining the lowest energy barrier for complex magnetic structures is highly complicated, with a complete multidimensional analysis feasible only for small systems with a particular set of magnetic parameters and geometry. On the other hand, a simpler semianalytical method using an analytical skyrmion ansatz [10,27] allows us to vary the micromagnetic and geometrical parameters rapidly. However, such an approach is bound to the ansatz symmetry and, therefore, only one energy barrier (corresponding to skyrmion contraction) is found. In the present paper, we expand the semianalytical method to account at least for three types of energy barriers for skyrmions in circular magnetic dots, corresponding to their collapse, expansion, and escape through the dot boundary. The magnetic field dependence of energy barriers for skyrmions in nanodots has not been investigated so far. The field dependence of the energy barriers is important for applications where a bias magnetic field is present. It allows us to characterize the dynamical coercivity and to easily evaluate its temperature dependence [28]. Here, we show that while at zero field, small skyrmions are typically unstable versus thermal fluctuations for ultrathin dots, the application of a magnetic field parallel to the skyrmion cores can stabilize them.

II. CALCULATION OF THE ENERGY BARRIERS

We study the energy barriers separating the skyrmion state from the (quasi)uniform state in a circular Co/Pt nanodot with strong interfacial Dzyaloshinskii-Moriya Interaction (DMI), which favors stabilization of the Néel skyrmions. The thickness L of the Co layer is 0.6 nm. We study the energy barriers as a function of the dot radius R and the intensity of the magnetic field B parallel to the symmetry axis of the dot. In our convention, positive magnetic fields are applied parallel to the skyrmion core, while negative ones are applied in the opposite direction [the studied system is depicted in Fig. 1(a)]. Note that in dots, the skyrmion stability and radius strongly depend on the dot size due to the finite-size (confinement) effect [9–11]. In particular, the skyrmion size can be smaller than that in a thin film with the same micromagnetic parameters.

We choose the magnetic parameters corresponding to an asymmetric Pt/Co/Pt multilayered system with a strong interfacial DMI between the Co/Pt layers [2], a saturation magnetization of $M_0 = 580$ kA/m, an exchange constant $A = 15$ pJ/m, a perpendicular anisotropy constant $K_u = 0.7$ MJ/m^3, and a DMI parameter of $D = 3$ mJ/m^2. In this system, the skyrmion is always a metastable state, that is, its energy is higher than that of the quasiuniform configuration. As has previously been shown in Ref. [10], the radius of the metastable skyrmion has a weak dependence

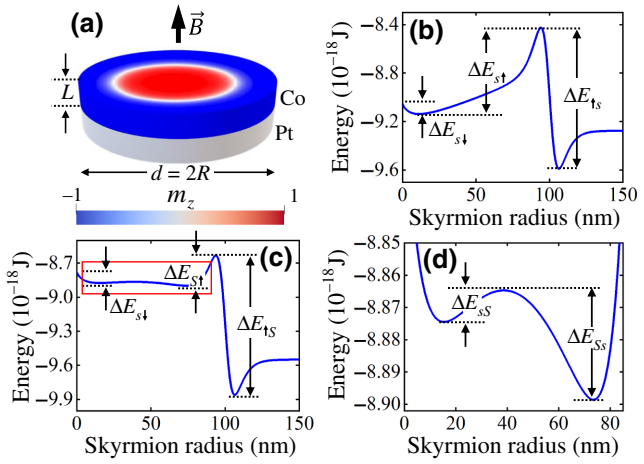

FIG. 1. (a) A skyrmion in the cylindrical nanodot at a magnetic field $\vec{B}$ pointing along the dot symmetry axis. The skyrmion energy as a function of the skyrmion radius R_s in a Pt/Co/Pt dot of radius 100 nm and thickness 0.6 nm, for (b) $B = 0$ and (c) $B = 25$ mT. (d) An enlargement of the bistability region in (c). We denote explicitly the energy barriers between the different magnetization states. The arrows indicate the energy barriers for skyrmion contraction $\Delta E_{s\downarrow}$, expansion $\Delta E_{s\uparrow}$, and between skyrmions of small and large diameter, ΔE_{sS} and ΔE_{Ss}, respectively.

on the magnetic field when it is applied out of plane, until it reaches some critical field, at which point the radius suddenly increases. The skyrmion is bistable if the bias magnetic field is close to this critical field, that is, a small and a large skyrmion can coexist within some range of the magnetic field values. Skyrmion-state bistability (the coexistence of small- and large-radius skyrmions) in thicker circular Co nanodots at zero magnetic field has also been predicted in Ref. [29]. The bistability is a result of competition between the DMI and the magnetostatic interaction increasing the dot thickness. In our case of ultrathin Co/Pt dots, the bistability results from a finite out-of-plane magnetic field within relatively narrow field intervals (shown later in Fig. 5).

We represent the Néel skyrmion energy profile E as a function of the skyrmion radius R_s for a skyrmion positioned in the dot center using an analytical ansatz for the skyrmion magnetization. In cylindrical coordinates (with the z axis directed parallel to the dot symmetry axis), the unit magnetization vector reads $\vec{m}(r, R_s) = m_z(r, R_s)\hat{z} + m_r(r, R_s)\hat{r}$, where $m_z = -\cos[\Theta_0(r, R_s)]$ and $m_r = \sqrt{1 - m_z^2}$, are written in terms of the $\Theta_0(r, R_s)$ function [30]:

$$\tan\left[\frac{\Theta_0(r, R_s)}{2}\right] = \frac{R_s}{r} e^{\xi(R_s - r)/l_{\rm ex}}. \qquad (1)$$

Here, r and $l_{\rm ex} = \sqrt{2A/\mu_0 M_0^2}$ are the radial cylindrical coordinate and the exchange length, respectively, and $\xi^2 = Q - 1$, where $Q = 2K_u/\mu_0 M_0^2$ is the quality factor. The trial ansatz of Eq. (1) has previously been used in Refs. [10,15] to evaluate the equilibrium skyrmion radius as a function of an applied magnetic field and as a function of the temperature, respectively, showing very good agreement with the direct numerical simulations.

We include in the magnetic energy functional E of the skyrmion an out-of plane uniaxial magnetic anisotropy, the exchange, magnetostatic, and Zeeman energies, and the interfacial Dzyaloshinskii-Moriya interaction:

$$E = \int_V dV \left(A \sum_{i=x,y,z} (\vec{\nabla} m_i)^2 - K_u m_z^2 - M_0 \vec{B} \cdot \vec{m} - \frac{\mu_0 M_0}{2} \vec{m} \cdot \vec{H}_d - D[m_z \vec{\nabla} \cdot \vec{m} - (\vec{m} \cdot \vec{\nabla}) m_z] \right), \qquad (2)$$

where μ_0 and $\vec{H}_d$ are the vacuum permeability and magnetostatic field, respectively. Note that all of the energy terms, except the magnetostatic one, are directly proportional to the dot thickness L.

For the calculation of the energy barriers for skyrmion escape via the dot boundary, we consider an off-center skyrmion. Therefore, it is convenient to use a coordinate system with its origin in the skyrmion core center (instead of a coordinate system with its origin in the dot center), as shown in Fig. 2(a). Also, we consider ultrathin dots and,

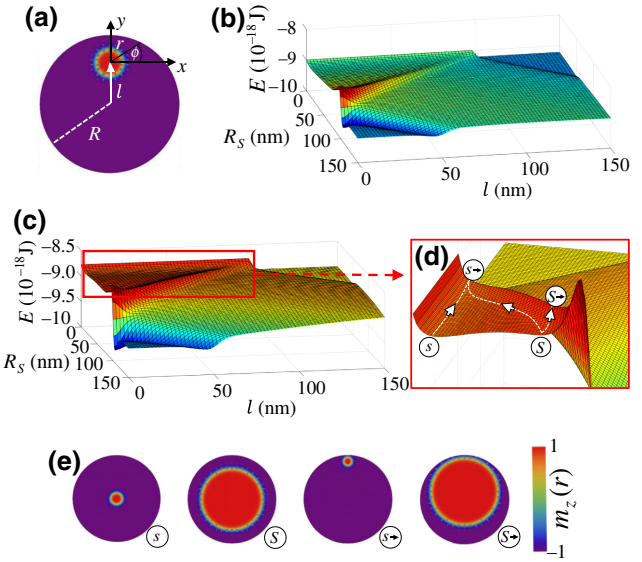

FIG. 2. (a) The scheme of a skyrmion with its center deviating a distance l from the dot center. The energy of a skyrmion as a function of the skyrmion radius and its deviation with respect to the dot center in a Pt/Co/Pt dot of $R = 100$ nm and thickness 0.6 nm, at (b) $B = 0$ and (c) $B = 20$ mT, respectively. (d) An enlargement showing the skyrmion energy [displayed in (c)], highlighting four magnetic configurations the snapshots of which appear in (e).

therefore, for this case we approximate the magnetostatic interaction as an easy-plane magnetic anisotropy, which can be included in the uniaxial anisotropy term by replacing the uniaxial anisotropy constant K_u by an effective uniaxial anisotropy constant $K_{\text{eff}} = K_u - \mu_0 M_0^2/2$ [11,31]. We also assume that the dot is thin enough and that the dot magnetization does not depend on the thickness coordinate, z. Therefore, due to the translational invariance along the z axis, we have to integrate the energy density in Eq. (2) over the dot surface,

$$E = L \begin{cases} \displaystyle\int_0^{2\pi} d\phi \int_0^{r_{\max}(\phi,l)} \mathcal{E}\, dr\, r, & l \le R, \\ \displaystyle\int_{l-R}^{l+R} dr\, r \int_{\phi_-(r,l)}^{\phi_+(r,l)} \mathcal{E}\, d\phi, & l > R, \end{cases} \tag{3}$$

where $r_{\max}(\phi, l) = -l\sin\phi + \sqrt{R^2 - l^2\cos^2\phi}$ and $\phi_\pm(r, l) = \pm\arccos[(r^2 + l^2 - R^2)/2rl] + 3\pi/2$. Note that by defining a coordinate system at the magnetic texture center, the displacement l of the skyrmion core from the dot center appears in the surface-integral limits [Eq. (3)]. The rigid skyrmion ansatz Eq. (1) is very good for calculating the energy barriers for centrosymmetric skyrmions. However, it cannot describe the possible deformations of the skyrmion shape when it approaches the dot border. In this case, the corresponding skyrmion energy will be overestimated.

The centrosymmetric energy barriers of the annihilation of the skyrmion by its core expansion and contraction can be obtained from the energy profile as a function of the skyrmion radius. Examples of several energy profiles as a function of the skyrmion radius are presented in Fig. 1 for a Co/Pt dot with radius $R = 100$ nm and at applied magnetic field values (b) 0 and (c) 25 mT. Note that the minimum of the energy profile at a skyrmion radius R_s located below the dot radius R corresponds to the skyrmion state, while the minimum of the energy located above the dot radius represents the quasisaturated state, with the net magnetization parallel to the skyrmion core magnetization. These two states are separated by the energy barrier of the skyrmion annihilation by expansion of its core, which we call $\Delta E_{s\uparrow}$. The energy functional is finite for $R_s \to 0$ corresponding to the finite value of the exchange energy for the ansatz Eq. (1) when $R_s \to 0$. This is since the studied ansatz in this limit coincides with the Belavin-Polyakov soliton ansatz, which is known to have a finite exchange energy independent of its radius [6]. The gap between this finite value and the energy of the skyrmion state with a finite radius corresponds to the energy barrier for the skyrmion annihilation by contraction of its radius, which we here call $\Delta E_{s\downarrow}$.

Furthermore, for $R = 100$ nm, the skyrmion states are bistable at high fields, as seen in Figs. 1(c) and 1(d) (as has been reported in Ref. [10]), with coexisting small- (s) and large- (S) radius metastable skyrmions. These two states are also separated by the energy barriers here called ΔE_{sS} and ΔE_{Ss}. In the particular case of Pt/Co/Pt, the bistability region spans approximately the field interval from 20 to 30 mT for dot radius $R = 100$ nm. The energy barriers separating these two states are quite small, approximately equal 5–10 $k_B T_0$, and the large skyrmion is more stable than the small one, i.e., it is separated by a larger barrier from a quasisaturated state. In agreement with this, in the presence of thermal fluctuations, the initial state in the form of a small skyrmion in Fig. 1(d) decays quickly at $B = 25$ mT to the skyrmion state of larger diameter. For a longer time scale at these fields, skyrmions are *superparamagnetic*, i.e., they spontaneously increase and decrease their radii between large and small values, thus exhibiting breathing behavior, and they stay longer in a state with a larger diameter. We note that in a typical situation shown in Fig. 1, the energy profile around the skyrmion minimum is very asymmetric and has a small curvature toward increasing radius. This means that under the influence of thermal fluctuations, the skyrmion increases its radius more easily than it decreases it.

On the other hand, an example of the energy profile as a function of the skyrmion radius and the displacement from the dot center is shown in Figs. 2(b), 2(c) for a Co/Pt dot of $R = 100$ nm for magnetic fields $B = 0$ and $B = 20$ mT, respectively. Figure 2(d) shows an enlargement of the energy profile at 20 mT, where four points of interest are explicitly highlighted, the snapshots of which are presented in Fig. 2(e). s and S correspond to skyrmions with a small and a large skyrmion radius, respectively, both centered in the dot, that is, with $l = 0$. Points $s \to$ and $S \to$ correspond to the critical points (saddle points), where the skyrmion core moves to the dot edge (with $l \neq 0$), for the small and large skyrmion radius, respectively. By fixing the magnetic and geometric parameters, the function $E(R_s, l)$ describes a surface in the configuration space where the saddle points separate the skyrmion states from the uniform states through displacement of the skyrmion center from the nanodot center. Note that the radius of the small skyrmion decreases when it escapes through the boundary while, on the contrary, the radius of the large one increases. The energy barrier associated with the annihilation of the skyrmion via its center displacement can be calculated by evaluating the minimum energy pass, i.e., the lowest difference of energies between the saddle-point energies and the skyrmion-state energies,

$$\Delta E_{s\to} = |\min[E(s\to), E(S\to)] - \min[E(s), E(S)]| \tag{4}$$

when the small or the large skyrmion state has the lowest energy, respectively. For the case of absence of the skyrmion bistability region [such as in Fig. 2(b)], there is only one skyrmion state.

III. RESULTS AND DISCUSSION

In Figs. 3(a)–3(c), we present the zero-field energy barriers as a function of the dot radius for the annihilation of the skyrmion by its center displacement, contraction, and expansion of its diameter, respectively. While the energy barriers for the skyrmion expansion are as large as 100 k_BT_0 at room temperature $T_0 = 300$ K, on the contrary, the energy barriers for the skyrmion contraction are of the order of 20 k_BT_0, while for the skyrmion escape they are small, of the order of 3 k_BT_0. We note that in all cases, the energy barrier for the skyrmion escape is the smallest one, which suggests that the skyrmion at zero field in an ultrathin dot will be quickly annihilated by its core displacement toward the dot edge. The decrease of the escape energy barrier for the dot radii above approximately 40 nm can be explained by the decrease of the confinement effect and dot curvature as the dot size increases. In this system, the skyrmion size has a weak dependence on the dot radius [10]. As the dot radius increases, the skyrmion practically maintains its size close to the dot border, whereas the effects of confinement and dot curvature decrease. Thus, it is easier for a skyrmion in an ultrathin Pt/Co/Pt dot to escape through a boundary of the dot of a larger size.

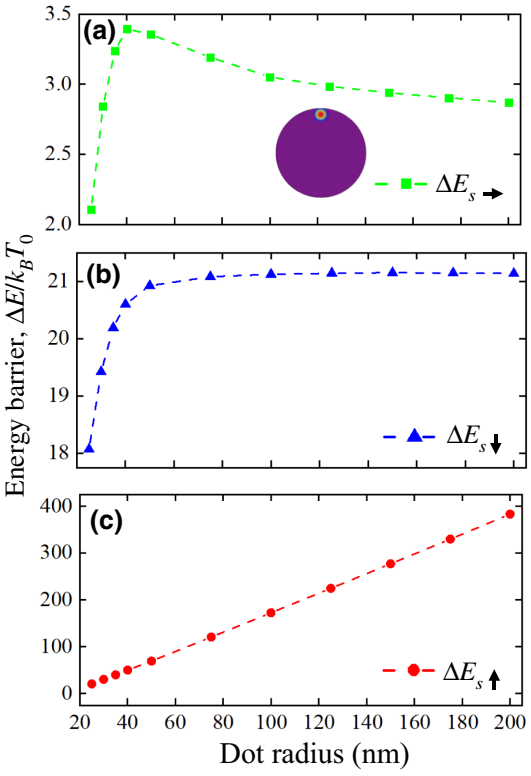

FIG. 3. The energy barriers at zero field for the annihilation of a skyrmion by (a) core displacement toward the dot edge, (b) core contraction, and (c) core expansion as a function of the dot radius for a Pt/Co/Pt dot of thickness 0.6 nm.

It is well known that the skyrmion ground states can be stabilized by external magnetic fields. This allows us to assume that external fields could also help to stabilize them with respect to thermal fluctuations, via the increase of the energy barriers. Thus, in the following we aim at evaluation of the energy barriers as a function of external fields. In Figs. 4 and 5, we show the three energy barriers for the annihilation of the skyrmion states as a function of the applied magnetic field for different values of the dot radius. Our first observation comes from the comparison between the skyrmion contraction and expansion: evidently, while for positive fields skyrmion expansion is more favorable, for negative fields it is skyrmion contraction, the transition being dependent on the dot radius. Most importantly, the results of Fig. 4(a) demonstrate a very different behavior of the escape barrier as a function of the dot size as compared to the zero-field case shown in Fig. 3(a). Namely, although this energy barrier remains the smallest one (except for

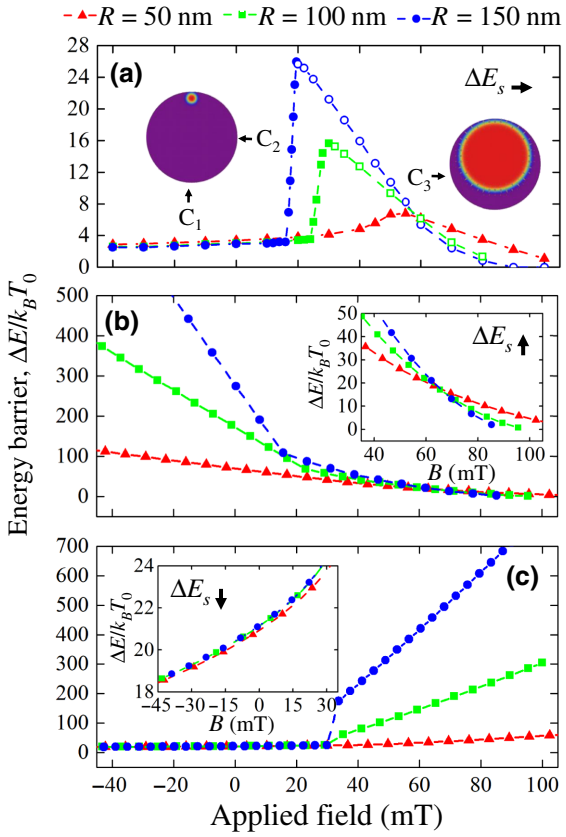

FIG. 4. The energy barriers of the annihilation of a skyrmion by (a) core displacement toward the dot edge, (b) core expansion, and (c) core contraction in a Pt/Co/Pt dot of thickness 0.6 nm and radius 50, 100, and 150 nm, as a function of the magnetic field applied in the out-of-plane z direction. The insets in (b) and (c) show the range where the energy barriers of core expansion and contraction are small. The solid symbols denote the energy barriers for the escape of the small skyrmion, while the open symbols are for that of the large one.

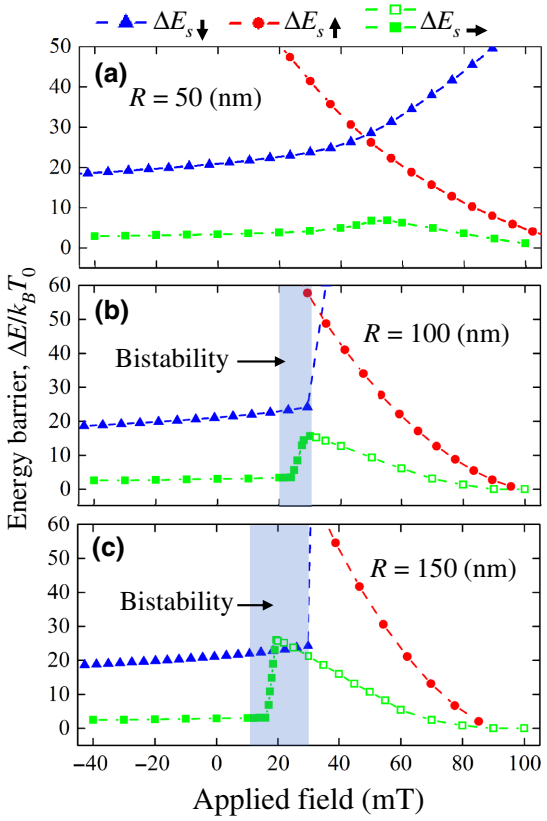

FIG. 5. The energy barriers for the skyrmion annihilation through the three studied mechanisms as a function of the magnetic field in a Pt/Co/Pt dot of thickness 0.6 nm when (a) $R = 50$, (b) $R = 100$, and (c) $R = 150$ nm. The bistability region, where the small radius skyrmion state s and the large radius skyrmion state S coexist, corresponds to the shaded region. Note that for $R = 50$ nm, there is no bistability region. The solid symbols denote the energy barrier for the escape of the small skyrmion, while the open symbols are for that of the large one.

the small region close to the field value of 20 mT, when $R = 150$ nm), there exists a range of positive external fields where it increases sufficiently to make the skyrmion stable for typical magnetometer measurements, i.e., reaching a lifetime with a duration of several seconds to several hours, depending on the prefactor f_0 of the Arrhenius law [20].

To better visualize the results of Fig. 4, in Fig. 5 we present the three energy barriers in the same plot for comparison of their magnitudes at low fields. The bistability region where the small skyrmion coexists with the large skyrmion is marked by the shaded region in Fig. 5. Note that the bistability region does not exist for the dot with a radius of 50 nm. The values of the energy barriers between the small and large skyrmion radius states calculated in Ref. [29] for thicker skyrmion dots are of several k_BT_0, which is in agreement with our simulations.

In Fig. 4(a), we define three types of skyrmion escape barriers, which we denote as C_1, C_2, and C_3. For the C_1 type, the minimum corresponds to the skyrmion with a small radius (s state) compared to the radius of the dot and also $\min[E(s\rightarrow), E(S\rightarrow)] = E(s\rightarrow)$, i.e., the skyrmion directly exits the dot while its radius decreases. As can be seen, this energy barrier is very small (less than 5 k_BT_0) and the skyrmion is very unstable in the C_1 region. On the contrary, for the C_2 region, as the applied magnetic field increases, the energy barrier increases strongly, until a critical value for which $\Delta E_{s\rightarrow}$ reaches its maximum. Interestingly, the transition between the C_1 and C_2 regimes occurs in the skyrmion bistability region when the skyrmion S of large radius exhibits less energy than the small radius skyrmion s. The bistability region is shown in detail in Fig. 6, where ΔE_{sS} and ΔE_{Ss} are the energy barriers that separate small skyrmion s from large skyrmion S and vice versa, respectively. In this figure, we explicitly denote by a vertical dashed line the transition between C_1 and C_2. Note that the energy barrier that separates the small- radius skyrmion s from the large-radius skyrmion S is very small in the C_2 region. Thus, the small-radius skyrmion is unstable in this region versus thermal fluctuations, so that it would first decay into the large-radius skyrmion. The opposite energy barrier from the large to the small skyrmion is quite large but still smaller than the direct escape of the large-radius skyrmion through the dot boundary. Consequently, in the C_2 region, the skyrmion

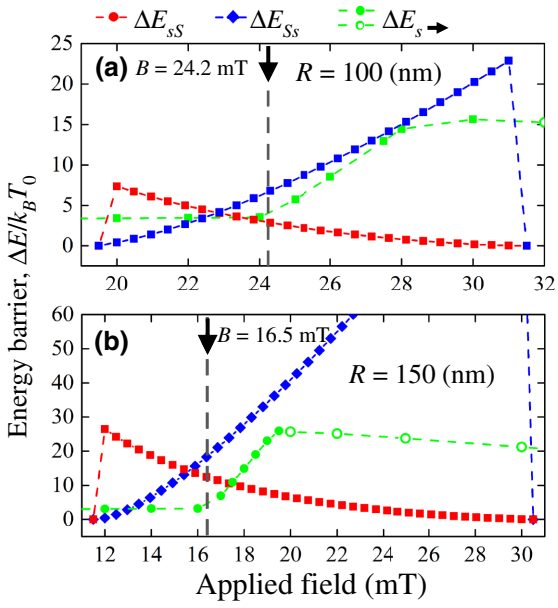

FIG. 6. The energy barriers between the small-radius and the large-radius skyrmion states, in the bistability region of the Pt/Co/Pt dot when (a) $R = 100$ nm and (b) $R = 150$ nm. For magnetic fields lower than those indicated by the dotted vertical line, the small skyrmion has less energy than the large skyrmion, while on the right, the opposite occurs. In order to compare the scale of the magnitude between the small energy barriers, we also include the field dependence of the barrier $\Delta E_{s\rightarrow}$.

exhibits a large radius and can be stable for hours before it is annihilated. Note that the actual skyrmion lifetime also depends on the Arrhenius-Néel prefactor [18,20]. It is important to note that as the radius of the dot increases, the skyrmion becomes more stable. When the thermal fluctuations are of the order of the energy barrier, the skyrmion S with a large core radius is annihilated first being converted to the small-radius skyrmion and then passing through the saddle point $s \rightarrow$. The skyrmion radius contracts as the skyrmion center deviates from the dot center until it is annihilated at the dot edge, following, for example, the path connecting S to the $s \rightarrow$ magnetization configurations [sketched in Fig. 2(d)].

In the C_3 region, which corresponds to magnetic field values larger than the critical value (where the barrier $\Delta E_{s\rightarrow}$ is maximal), the energy barrier of annihilation of the skyrmion by its center displacement decreases as the magnetic field increases. In addition, the skyrmion has a large core radius and it holds that $\min[E(s \rightarrow), E(S \rightarrow)] = E(S \rightarrow)$, showing that when the thermal fluctuations are comparable with the energy barrier of the skyrmion displacement, the skyrmion is annihilated by the deviation of its center directly by the escape of the large-size skyrmion through the dot boundary [following, for example, the trajectory connecting S to $S \rightarrow$, sketched in Fig. 2(d)]. In order to distinguish the cases when the skyrmion escapes through the dot edge with a small or large core radius for the dot sizes that exhibit a bistability region, we use solid and open symbols in the $\Delta E_{s\rightarrow}$ curves when the skyrmion escapes with a small and a large core radius, respectively. Note that in the C_1 and C_2 field regions, when thermal fluctuations destroy the skyrmion stability, the skyrmion escapes with a small skyrmion radius, while in the C_3 region it escapes with a large skyrmion radius. Thus, the maximum of the lowest energy barrier in Figs. 4(a) and 5 corresponds to the change of the skyrmion lowest-energy pass from the escape of the small skyrmion to the escape of the large skyrmion. While in the former case the energy barrier increases with the increasing out-of-plane magnetic field (until some critical field at which it starts to decrease), in the latter case it decreases. In simple words, a small skyrmion becomes more stable with an increasing magnetic field because its size increases, while the large one becomes less stable because it is more sensitive to the boundary. Consequently, there is an optimal skyrmion radius (defined by the bias magnetic field value) that corresponds to the optimal energy barrier.

For completeness, with the aim of showing that the proposed method can be applied to obtain the energy barriers in different magnetic systems, in the Appendix we show the behavior of the three energy barriers in Pt/Co/Ni or Ir/Co/Pt ultrathin multilayered dots. These results show similar behavior of the three energy barriers, both as a function of the dot radius and as a function of the applied out-of-plane magnetic field for the annihilation of magnetic skyrmions in a Pt/Co/Ni multilayered dot. The similarity of the behavior of the energy barriers in Pt/Co/Pt and Pt/Co/Ni agrees with the universal behavior of skyrmions in both systems reported in Ref. [10]. Indeed, in this reference it is shown that in both systems, the skyrmion is small and metastable at zero field and can show a bistability region for certain values of the field. On the other hand, skyrmions in Ir/Co/Pt are stable at zero field and do not show a bistability region. In particular, skyrmions there have a large core and a similar behavior to the large-core skyrmions in the transition region for the Pt/Co/Pt case. The lowest energy barrier again corresponds to the annihilation of the skyrmion by escape through the dot border. However, the skyrmions in a Ir/Co/Pt system should be stable versus thermal fluctuations even at zero field in dots with a radius of approximately 200 nm and above and can be slightly stabilized by fields applied parallel to their core magnetizations.

IV. CONCLUSIONS

In summary, we calculate three energy barriers that separate the skyrmion states from the quasiuniform magnetization state in ultrathin circular Pt/Co/Pt nanodots, as a function of the out-of-plane magnetic field for different dot radii. At zero field, the energy barrier for the annihilation of the skyrmion by its core displacement has a small value and is always the lowest energy barrier. Therefore, the skyrmion annihilates at the dot edge (due to the skyrmion core escaping from the dot). We find that one can stabilize skyrmions by applying an out-of-plane magnetic field parallel to their core magnetization. In our case, this happens for magnetic field values close to 20 mT in a Pt/Co/Pt dot of radius 150 nm, in which the energy barrier for the skyrmion contraction is even lower than the energy barrier for the skyrmion core displacement [see Fig. 5(c)]. In this case, the skyrmion can be stable for hours until it annihilates due to its core contraction. The skyrmion stabilization occurs in the bistability region when both small- and large-radius skyrmions are stable (metastable) states confined by the dot boundary. In this region, the large-radius skyrmion is stable versus thermal fluctuations and is separated by an energy barrier of the order of 20 $k_B T_0$ from the small-radius skyrmion. The lowest energy pass goes through conversion of the large skyrmion to the small one and then via the escape of the small skyrmion over the energy barrier.

Our model is sufficiently general and can be extended to perform a systematic study over several magnetic materials; for example, as a function of the DMI constant, exchange stiffness, or saturation magnetization values. In the Appendix, we also investigate ultrathin Pt/Co/Ni and Ir/Co/Pt dots, also showing that the lowest energy barrier corresponds to skyrmion annihilation by escape through the dot boundary.

On the other hand, since the ansatz [Eq. (1)] used for the calculation of the three energy barriers corresponds to a rigid skyrmion-magnetization configuration, the results of the energy barrier for core deviation do not allow us to estimate the deformation of the skyrmion core as the core reaches the dot edge. Nevertheless, as any trial function of the magnetization configuration, like the ansatz of Eq. (1), leads to overestimation of the configuration energy, we expect that the energy barriers including core deformation are higher than those estimated analytically within the rigid skyrmion model (since the minimized skyrmion energy will be lower than that given by a rigid skyrmion model).

It is worth mentioning that, frequently, the energy-barrier evaluation is sufficient for skyrmion thermal stability assessment in technological applications based on the order of magnitude of the Arrhenius prefactor (the attempt frequency). However, recently a large variation of the prefactor, by several orders of magnitude, has been reported for skyrmions, which shows the necessity of correct evaluation of the attempt frequency [20,32,33]. It has been shown in Ref. [32] that the attempt frequency for skyrmion collapse decreases with the applied magnetic field for fcc stackings such as in Pd/Fe/Ir and fcc Pd/Fe/Rh systems, enhancing the lifetime stability as a function of the field strength in these systems. Instead, for hcp arrangements, the attempt frequency increases with the intensity of the field. On the other hand, the behavior of the attempt frequency also depends on the mechanism for skyrmion annihilation. It has been shown in Ref. [33] that the attempt frequency for skyrmion collapse (contraction of its core) changes by several orders of magnitude with the applied magnetic field, while the attempt frequency for skyrmion annihilation by its core displacement has a weak dependence on the applied magnetic field. Additionally, the change in magnitude for the attempt frequency for skyrmion collapse appears for variation in the magnetic field of a few teslas, while in our work the applied field varies within the narrow interval from -40 to 100 mT. The above indicates that the assumption of a constant field-independent prefactor can be reasonable for our case. However, to clarify the complete picture of skyrmion lifetimes, the behavior of the attempt frequency requires further study.

We would like to point out that our findings related to the lowest energy barrier given by the skyrmion exit through the dot border will be important for the design of skyrmion applications in confined nanostructures. In particular, it is expected that in skyrmion-based racetrack memories [34], the lowest energy barrier may also be that of the skyrmion expelled from the stripe. The calculated values of the energy barriers in circular magnetic dots of non-small radius suggest that it is possible to stabilize the skyrmion versus thermal fluctuations in ultrathin dots by an external out-of-plane magnetic field. This opens an opportunity for experimental measurements of the skyrmion dynamics in ultrathin dots not solely at low temperatures, when the thermal fluctuations are suppressed. We note that the relaxation times and energy barriers of strongly inhomogeneous magnetization configurations such as skyrmions or vortices can be found either by direct measurement of the in-field magnetic viscosity [35] or by measuring the time-dependent intensities of the broadband ferromagnetic resonance peaks [36]. The field dependence of the energy barriers is also an important characteristic of dynamical coercivity [37,38]. The energy-barrier values can be further optimized by varying the magnetic and geometrical parameters of the system.

ACKNOWLEDGMENTS

We acknowledge financial support from the CONICYT + PAI/Convocatoria Nacional Subvención a la instalación en la Academia, convocatoria 2019 + Folio 77190042, ANID-PFCHA/Postdoctorado Becas Chile 74200122, Dicyt-Usach Grant No. 041931EM-POSTDOC, FONDECYT Grant No. 1200302 and Basal Project AFB180001. K.G. acknowledges support by Ikerbasque, the Basque Foundation for Science. The work of K.G. and O.C.-F. was supported by the Spanish Ministry of Science and Innovation under Grants No. FIS2016-78591-C3-3-R, No. PID2019-108075RB-C31, and No. PID2019-108075RB-C33/AEI/10.13039/501100011033.

APPENDIX: ENERGY BARRIERS FOR SKYRMION ANNIHILATION IN ULTRATHIN Pt/Co/Ni and Ir/Co/Pt MULTILAYERED DOTS

With an aim of showing that the proposed method for the calculation of the energy barriers of the annihilation of the magnetic skyrmions can be straightforwardly applied to several magnetic systems, in this Appendix we calculate the energy barriers for the three studied mechanisms for annihilation of magnetic skyrmions in ultrathin Pt/Co/Ni and Ir/Co/Pt multilayered dots (for the same dot thickness $L = 0.6$ nm as studied for Pt/Co/Pt dots). The magnetic parameters of these systems are taken from Refs. [25,39] and are given in Table I.

In Fig. 7, we show the energy barriers at zero magnetic field as a function of the dot radius for the annihilation

TABLE I. The parameters for the Pt/Co/Ni and Ir/Co/Pt circular multilayered dots.

Magnetic parameters	Pt/Co/Ni	Ir/Co/Pt
Saturation magnetization, M_0 (kA/m)	600	956
Exchange constant, A (pJ/m)	20	10
Perpendicular anisotropy constant, K_u (MJ/m^3)	0.6	0.717
DMI parameter, D (mJ/m^2)	3	1.6

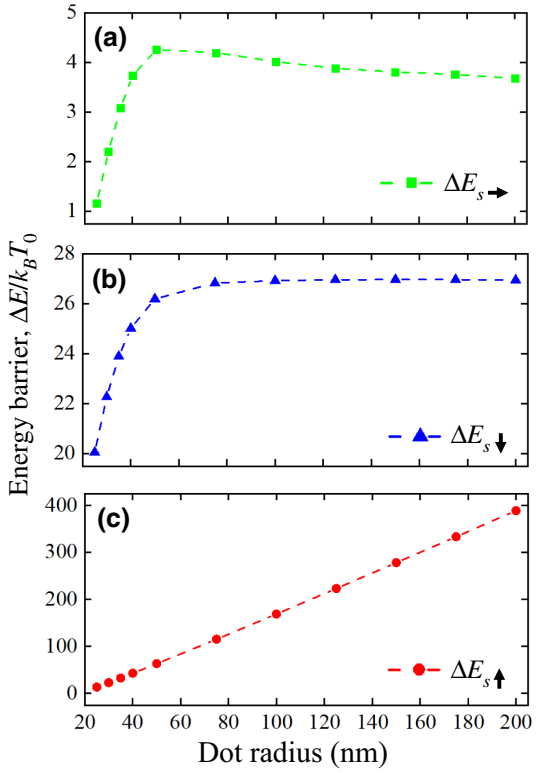

FIG. 7. The energy barriers at zero field as a function of the dot radius for skyrmion annihilation by (a) deviation, (b) contraction, and (c) expansion of its core in Pt/Co/Ni dots.

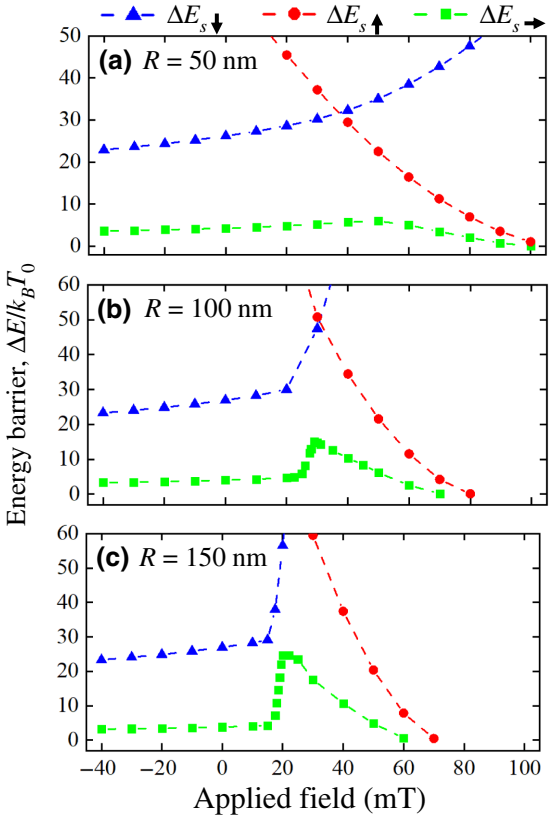

FIG. 8. The energy barriers as a function of the out-of-plane magnetic field for skyrmion annihilation in a Pt/Co/Ni dot of radius (a) $R = 50$, (b) 100, and (c) 150 nm.

of the magnetic skyrmion in a Pt/Co/Ni dot for the three mechanisms: (a) by core deviation, (b) by core contraction, and (c) by core expansion. As can be seen, the behavior of the three energy barriers are similar to those shown in Fig. 3. Indeed, like the barrier calculated for Pt/Co/Pt, the lower energy barrier at zero field is small in Pt/Co/Ni dot, below 5 k_BT_0, and corresponds to the annihilation of the skyrmion by core displacement and its escape from the dot.

On the other hand, the energy barriers as a function of the out-of-plane magnetic field for Pt/Co/Ni are shown in Fig. 8. Again, by comparing with Fig. 5, similar behavior of the energy barriers for the three dot sizes can be observed. The similarity of the behavior of the energy barriers for skyrmion annihilation in Pt/Co/Pt and Pt/Co/Ni dots agrees with the universal behavior of metastable small magnetic skyrmions at zero magnetic field shown in Ref. [10]. Indeed, both the Pt/Co/Pt and Pt/Co/Ni systems show a small-radius skyrmion, which is metastable at zero field. Additionally, both systems also reveal a bistability region for dot radius $R = 100$ and 150 nm in which a small-radius skyrmion and a large-radius skyrmion coexist for certain values of an applied magnetic field. Moreover, as in a Pt/Co/Pt dot, the bistability region in the Pt/Co/Ni dot allows to increase the value of the lower energy barrier to the values close to and above 20 k_BT_0, for the dot radii 100 and 150 nm, respectively.

Now, we analyze the behavior of the three energy barriers in a different magnetic system, an Ir/Co/Pt dot, which shows a different universal magnetic skyrmion behavior. Unlike the Pt/Co/Pt and Pt/Co/Ni systems, the skyrmion in

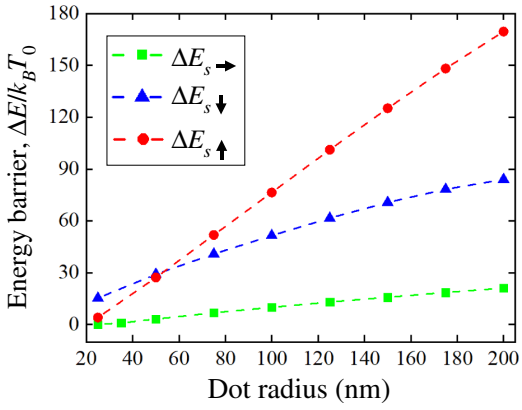

FIG. 9. The energy barriers at zero field as a function of the dot radius for skyrmion annihilation by the three studied mechanisms in Ir/Co/Pt dots.

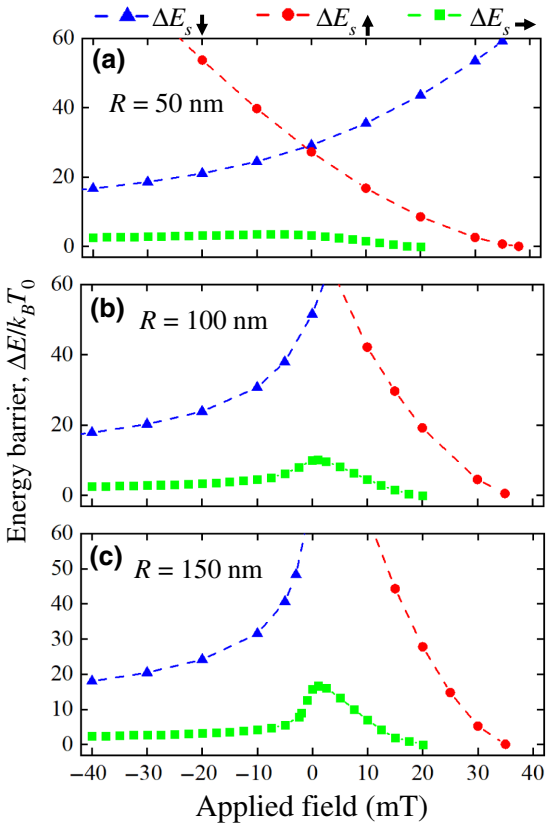

FIG. 10. The energy barriers as a function of the out-of-plane magnetic field for skyrmion annihilation in Ir/Co/Pt dots of radius (a) $R = 50$, (b) 100, and (c) 150 nm.

a Ir/Co/Pt is large and stable at zero field and does not show a bistability region in the presence of an out-of-plane magnetic field [10]. In Figs. 9 and 10, we show the behavior of the three energy barriers for a skyrmion in this magnetic material as a function of the dot radius at zero field and as a function of the out-of-plane field, respectively. Unlike the previous cases, all energy barriers increase as a function of the dot radius. As in the previously studied materials, the lowest energy barrier corresponds to annihilation by core displacement from the dot center. However, for the dots with a radius of approximately 200 nm and above, this energy barrier has a reasonable value that ensures skyrmion thermal stability at zero field. As a function of the out-of-plane magnetic field, the energy barriers have qualitatively the same behavior as in the above cases. The lowest energy barrier is a maximum close to zero field and can be increased slightly by applying a magnetic field parallel to the skyrmion core.

[1] A. Fert, V. Cros, and J. Sampaio, Skyrmions on the track, Nat. Nanotechnol. **8**, 152 (2013).
[2] J. Sampaio, V. Cros, S. Rohart, A. Thiaville, and A. Fert, Nucleation, stability and current-induced motion of isolated magnetic skyrmions in nanostructures, Nat. Nanotechnol. **8**, 839 (2013).
[3] X. Zhang, M. Ezawa, and Y. Zhou, Magnetic skyrmion logic gates: Conversion, duplication and merging of skyrmions, Sci. Rep. **5**, 9400 (2015).
[4] W. Kang, Y. Huang, C. Zheng, W. Lv, N. Lei, Y. Zhang, X. Zhang, Y. Zhou, and W. Zhao, Voltage controlled magnetic skyrmion motion for racetrack memory, Sci. Rep. **6**, 23164 (2016).
[5] N. Vidal-Silva, A. Riveros, F. Tejo, J. Escrig, and D. Altbir, Controlling the nucleation and annihilation of skyrmions with magnetostatic interactions, Appl. Phys. Lett. **115**, 082405 (2019).
[6] A. M. Kosevich, B. Ivanov, and A. S. Kovalev, Magnetic solitons, Phys. Rep. **194**, 117 (1990).
[7] A. R. Aranda and K. Y. Guslienko, Single chiral skyrmions in ultrathin magnetic films, Materials **11**, 2238 (2018).
[8] J. Wild, T. N. G. Meier, S. Pollath, M. Kronseder, A. Bauer, A. Chacon, M. Halder, M. Schowalter, A. Rosenauer, J. Zweck, J. Muller, A. Rosch, C. Pfleiderer, and C. H. Back, Entropy-limited topological protection of skyrmions, Sci. Adv. **3**, e1701704 (2017).
[9] A. R. Aranda, A. Hierro-Rodriguez, G. N. Kakazei, O. Chubykalo-Fesenko, and K. Y. Guslienko, Magnetic skyrmion size and stability in ultrathin nanodots accounting Dzyaloshinskii-Moriya exchange interaction, J. Magn. Magn. Mater. **465**, 471 (2018).
[10] F. Tejo, A. Riveros, J. Escrig, K. Y. Guslienko, and O. Chubykalo-Fesenko, Distinct magnetic field dependence of Néel skyrmion sizes in ultrathin nanodots, Sci. Rep. **8**, 6280 (2018).
[11] S. Rohart and A. Thiaville, Skyrmion confinement in ultrathin film nanostructures in the presence of Dzyaloshinskii-Moriya interaction, Phys. Rev. B **88**, 184422 (2013).
[12] K. Y. Guslienko, Néel skyrmion stability in ultrathin circular magnetic nanodots, Appl. Phys. Express **11**, 063007 (2018).
[13] N. Vidal-Silva, A. Riveros, and J. Escrig, Stability of Neel skyrmions in ultra-thin nanodots considering Dzyaloshinskii-Moriya and dipolar interactions, J. Magn. Magn. Mater. **443**, 116 (2017).
[14] A. Riveros, N. Vidal-Silva, F. Tejo, and J. Escrig, Analytical and numerical K_u-B phase diagrams for cobalt nanostructures: Stability region for a Bloch skyrmion, J. Magn. Magn. Mater. **460**, 292 (2018).
[15] R. Tomasello, K. Y. Guslienko, M. Ricci, A. Giordano, J. Barker, M. Carpentieri, O. Chubykalo-Fesenko, and G. Finocchio, Origin of temperature and field dependence of magnetic skyrmion size in ultrathin nanodots, Phys. Rev. B **97**, 060402(R) (2018).
[16] G. Mills, H. Jonsson, and G. Schenter, Reversible work transition state theory: Application to dissociative adsorption of hydrogen, Surf. Sci. **324**, 305 (1995).
[17] H. Jonsson, G. Mills, and K. W. Jacobsen, in *Classical and Quantum Dynamics in Condensed Phase Simulations*, edited by B. J. Berne, G. Ciccotti, and D. F. Coker (World Scientific, Singapore, 1998), p. 385.
[18] P. F. Bessarab, V. M. Uzdin, and H. Jonsson, Method for finding mechanism and activation energy of magnetic transitions, applied to skyrmion and antivortex annihilation, Comput. Phys. Commun. **196**, 335 (2015).

[19] D. Cortes-Ortuño, W. Wang, M. Beg, R. A. Pepper, M.-A. Bisotti, R. Carey, M. Vousden, T. Kluyver, O. Hovorka, and H. Fangohr, Thermal stability and topological protection of skyrmions in nanotracks, Sci. Rep. **7**, 4060 (2017).

[20] L. Desplat, D. Suess, J.-V. Kim, and R. L. Stamps, Thermal stability of metastable magnetic skyrmions: Entropic narrowing and significance of internal eigenmodes, Phys. Rev. B **98**, 134407 (2018).

[21] I. S. Lobanov, H. Jonsson, and V. M. Uzdin, Mechanism and activation energy of magnetic skyrmion annihilation obtained from minimum energy path calculations, Phys. Rev. B **94**, 174418 (2016).

[22] S. Rohart, J. Miltat, and A. Thiaville, Path to collapse for an isolated Néel skyrmion, Phys. Rev. B **93**, 214412 (2016).

[23] E. Paz, F. Garcia-Sanchez, and O. Chubykalo-Fesenko, Numerical evaluation of energy barriers in nano-sized magnetic elements with Lagrange multiplier technique, Physica B: Condens. Matter **403**, 330 (2008).

[24] J. Hagemeister, N. Romming, K. von Bergmann, E. Y. Vedmedenko, and R. Wiesendanger, Stability of single skyrmionic bits, Nat. Commun. **6**, 8455 (2015).

[25] C. Moreau-Luchaire, C. Moutafis, N. Reyren, J. Sampaio, C. A. F. Vaz, N. Van Horne, K. Bouzehouane, K. Garcia, C. Deranlot, P. Wohlhuter, J.-M. George, M. Weigand, J. Raabe, V. Cros, and A. Fert, Additive interfacial chiral interaction in multilayers for stabilization of small individual skyrmions at room temperature, Nat. Nanotech. **11**, 444 (2016).

[26] A. Fert, N. Reyren, and V. Cros, Magnetic skyrmions: Advances in physics and potential applications, Nat. Rev. Mater. **2**, 17031 (2017).

[27] F. Buttner, I. Lemesh, and G. S. D. Beach, Theory of isolated magnetic skyrmions: From fundamentals to room temperature applications, Sci. Rep. **8**, 4464 (2018).

[28] F. Garcia-Sanchez and O. Chubykalo-Fesenko, Thermal coercivity mechanism in Fe nanoribbons and stripes, Appl. Phys. Lett. **93**, 192508 (2008).

[29] M. Zelent, J. Tobik, M. Krawczyk, K. Y. Guslienko, and M. Mruczkiewicz, Bi-stability of magnetic skyrmions in ultrathin multilayer nanodots induced by magnetostatic interaction, Phys. Status Solidi RRL **11**, 1700259 (2017).

[30] W. J. DeBonte, Properties of thick-walled cylindrical magnetic domains in uniaxial platelets, J. Appl. Phys. **44**, 1793 (1973).

[31] G. Gioia and R. D. James, Micromagnetics of very thin films, Proc. R. Soc. Lond. A **453**, 213 (1997).

[32] S. von Malottki, P. F. Bessarab, S. Haldar, A. Delin, and S. Heinze, Skyrmion lifetime in ultrathin films, Phys. Rev. B **99**, 060409(R) (2019).

[33] P. F. Bessarab, G. P. Muller, I. S. Lobanov, F. N. Rybakov, N. S. Kiselev, H. Jonsson, V. M. Uzdin, S. Blugel, L. Bergqvist, and A. Delin, Lifetime of racetrack skyrmions, Sci. Rep. **8**, 3433 (2018).

[34] R. Tomasello, E. Martinez, R. Zivieri, L. Torres, M. Carpentieri, and G. Finocchio, A strategy for the design of skyrmion racetrack memories, Sci. Rep. **4**, 6784 (2014).

[35] G. N. Kakazei, M. Ilyn, O. Chubykalo-Fesenko, J. Gonzalez, A. A. Serga, A. V. Chumak, P. A. Beck, B. Laegel, B. Hillebrands, and K. Y. Guslienko, Slow magnetization dynamics and energy barriers near vortex state nucleation in circular permalloy dots, Appl. Phys. Lett. **99**, 052512 (2011).

[36] G. A. Melkov, Y. Kobljanskyj, V. Novosad, A. N. Slavin, and K. Y. Guslienko, Probing the energy barriers in nonuniform magnetization states of circular dots by broadband ferromagnetic resonance, Phys. Rev. B **88**, 220407 (2013).

[37] M. P. Sharrock, Time dependence of switching fields in magnetic recording media, J. Appl. Phys. **76**, 6413 (1994).

[38] Y. K. Takahashi, K. Hono, S. Okamoto, and O. Kitakami, Magnetization reversal of FePt hard/soft stacked nanocomposite particle assembly, J. Appl. Phys. **100**, 074305 (2006).

[39] K. S. Ryu, S.-H. Yang, L. Thomas, and S. S. P. Parkin, Chiral spin torque arising from proximity-induced magnetization, Nat. Commun. **5**, 3910 (2014).